

# Heralded Photonic Interaction between Distant Single Ions

M. Schug<sup>1,\*</sup>, J. Huwer<sup>1,2</sup>, C. Kurz<sup>1</sup>, P. Müller<sup>1</sup>, and J. Eschner<sup>1</sup>

<sup>1</sup>*Universität des Saarlandes, Experimentalphysik, Campus E2 6, 66123 Saarbrücken, Germany*

<sup>2</sup>*ICFO – The Institute of Photonic Sciences, Avenida Carl Friedrich Gauss 3, 08860 Castelldefels (Barcelona), Spain*

(Dated: October 26, 2018)

We establish a heralded interaction between two remotely trapped single  $^{40}\text{Ca}^+$  ions through the exchange of single photons. In the sender ion, we release single photons with a controlled temporal shape on the  $P_{3/2}$  to  $D_{5/2}$  transition and transmit them to the distant receiver ion. Individual absorption events in the receiver ion are detected by quantum jumps. For continuously generated photons, the absorption reduces significantly the lifetime of the long-lived  $D_{5/2}$  state. For triggered single-photon transmission, we observe a coincidence between the emission at the sender and quantum jump events at the receiver.

PACS numbers: 42.50.Ex, 42.50.Ct, 03.67.Hk, 42.50.Dv

The realization of quantum networks requires the controlled transfer of quantum states between quantum systems in a reversible manner, allowing for the distribution of entanglement across the network [1]. One proposed experimental implementation of such a network consists of single atoms as nodes, where quantum information is stored and processed, and single photons for direct transmission between the nodes [2]. In this context, it is a main prerequisite to control both the emission and absorption of single photons by spatially separated single atoms or atom-like systems.

For controlled single-photon emission, various systems exist [3] such as neutral atoms [4, 5], trapped ions [6, 7], or solid state systems [8, 9], which offer tailoring of specific properties of the emitted photons. Beyond that, entanglement between a quantum system and its emitted photons [10–13] paves the way to transferring quantum information between distant network nodes. These nodes may serve as bi-directional quantum interfaces, provided that also control over the absorption of single photons by a single atom is attained [2]. In this context, we have demonstrated the heralded photon absorption by a single ion [14, 15]. Controlling both the emission and absorption is approached in recent experiments with two single quantum emitters such as organic molecules [16] or atoms in optical cavities [17, 18]. Scalability of quantum networks to long distance quantum communication is enabled by heralded entanglement between widely spaced atoms [19, 20], and exploiting the quantum repeater scheme [21]. Additionally, hybrid systems between different physical systems, such as entangled-photon sources and ions [14, 15], entangled photons and quantum dots [22], or atoms and ions [23], may be deployed to create building blocks of quantum repeater systems.

Single trapped ions are ideal nodes for quantum networks, being particularly well controlled in their motional and internal degrees of freedom and thereby allowing for coherent processing of quantum information. Communication by photon transmission between distant ions re-

quires creation of single photons with controlled temporal shape and coherence time [24], ideally in a pure quantum state [13, 25]; at the same time, absorption of single photons must happen in a deterministic or heralded manner [14, 15, 25] in order to map the photonic state to the ion. Such individual discrimination of absorption events has not been implied in previous experiments [16–18].

In this letter we report the heralded interaction between distant single ions by emission and absorption of individual photons. We perform photon transmission in continuous and sequence mode. Most importantly, individual absorption events are detected by quantum jumps, and coincidence between the photon generation and the absorption event is demonstrated.

Fig. 1a shows the double-trap apparatus consisting of two linear Paul traps separated by approximately one meter. In each trap a single  $^{40}\text{Ca}^+$  ion is confined and excited by various laser beams for cooling and state manipulation. Along one of the axes, two in-vacuum high numerical aperture laser objectives (HALOs) provide efficient optical access to the ions [26]. In the sender ion trap we generate single 854 nm photons of which we collect about 4% with one HALO. We couple the photons into a single-mode fiber that connects the two traps. In the receiver ion trap we use one HALO to couple the 854 nm photons to the ion, and the other one to collect 397 nm fluorescence photons which are detected with a photomultiplier tube (PMT).

The laser excitation scheme of the sender ion is illustrated in Fig. 1b. For triggered generation of single 854 nm photons, the sequence starts with Doppler cooling using laser light at 397 nm and 866 nm. Subsequently, an 850 nm laser couples the  $D_{3/2}$  to the  $P_{3/2}$  level, thereby optically pumping the ion to the  $D_{5/2}$  level and triggering the emission of a single 854 nm photon. The beginning of the 850 nm laser pulse is used as a time stamp, i.e. as a herald, for the photon generation. Finally, an 854 nm laser repumps the ion to the  $S_{1/2}$  level and concludes the sequence. For continuous generation of 854 nm photons, all four lasers are constantly switched on.

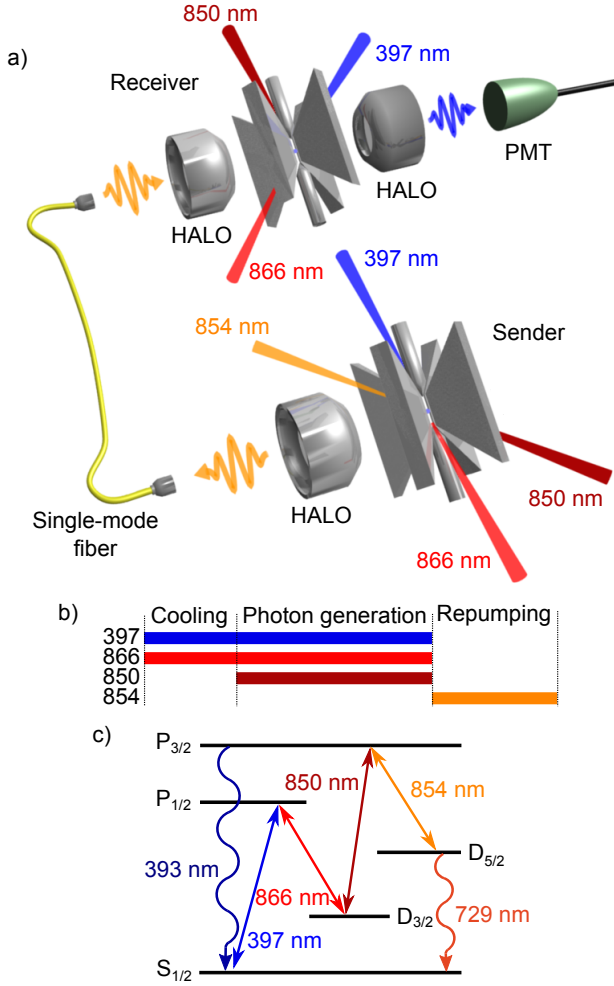


FIG. 1. (Color online) a) Schematic of the apparatus consisting of two linear Paul traps separated by one meter distance and connected by a single-mode fiber. b) Laser excitation scheme for triggered single-photon generation at the sender ion; see text for more details. c) Level scheme and relevant transitions of the  $^{40}\text{Ca}^+$  ion. The  $P_{3/2}$  level decays with  $2\pi \cdot 21.49$  MHz to  $S_{1/2}$  and with  $2\pi \cdot 1.35$  MHz to  $D_{5/2}$  [27]; the lifetime of the  $D_{5/2}$  level is 1.1 s.

At the receiver ion, continuous-wave (cw) excitation with three lasers initializes the absorption of 854 nm photons: the 397 nm and 866 nm lasers Doppler cool the ion, while the emitted 397 nm fluorescence is monitored, and an attenuated 850 nm laser optically pumps the ion to the metastable  $D_{5/2}$  level. A quantum jump to that level is marked by a sudden drop of the 397 nm fluorescence signal to the dark-count rate (a bright-to-dark quantum jump). In the  $D_{5/2}$  state the ion can absorb a photon from the sender, which excites it to  $P_{3/2}$ . Subsequent decay to  $S_{1/2}$  (with 93.47% probability [27]) is accompanied by the onset of the fluorescence (a dark-to-bright quantum jump) which thus signals the absorption. Such a quantum jump may also be caused by a spontaneous decay from  $D_{5/2}$  to  $S_{1/2}$ . In the following, this quan-

tum jump scheme is used to observe and characterize the interaction of the two ions via triggered and continuous transmission of photons.

Since we aim at high-rate interaction between the ions, we first optimize the efficiency of the single photon generation at the sender ion, i.e. of the optical pumping process into the  $D_{5/2}$  level. We find that by employing a three-photon resonance condition for the three lasers that connect  $S_{1/2}$  and  $P_{3/2}$  (397 nm, 866 nm, and 850 nm, see Fig. 1c), the pumping rate is significantly increased over the one that would be achieved by consecutive optical pumping (corresponding to using only the 397 nm and 850 nm lasers). This is corroborated by comparing the rates of scattered photons at 393 nm and 397 nm,  $R_{393}$  and  $R_{397}$ , during the pumping: consecutive optical pumping would yield  $R_{393}/R_{397} = 0.065$ , equal to the branching ratio of  $P_{1/2}$  into  $D_{3/2}$  (after correcting for different detection efficiencies at the two wavelengths). Our optimized scheme yields, in cw excitation conditions,  $R_{393}/R_{397} = 1.34(2)$ , hence the coherent three-photon process enhances the photon generation rate by a factor of 20. Using such optimized excitation parameters, we measure  $4.5 \cdot 10^3 \text{ s}^{-1}$  fiber-coupled 854 nm photons using an avalanche photodiode (APD) with 24(5)% detection efficiency. From this we derive a continuous generation rate  $R_{854, \text{cw}} = 18(4) \text{ kHz}$  of 854 nm photons in a single optical mode.

In order to further characterize the single photons for the sender-receiver interaction, we excite the sender ion to generate triggered single photons in sequence mode. The photons are collected in a single-mode fiber, and their arrival times on an APD are recorded with respect to the onset of the 850 nm laser pulse that triggers the emission. Fig. 2 displays the arrival time distributions, i.e. the shapes of the respective single-photon wave packets, for various power values of the 850 nm laser. Variation of the 850 nm laser power allows us to control the wave packet duration  $T_1$  (defined as the  $1/e$  arrival time) between  $0.83(3) \mu\text{s}$  and  $5.8(5) \mu\text{s}$  [28]. We note that in contrast to the work of Refs. [24, 25], the photon wave packets of Fig. 2 are incoherently broadened, i.e. the photons are far from Fourier-limited, because of the unfavorable branching ratio of the  $P_{3/2}$  level. For the shortest measured photons, and for 125 kHz repetition rate of the pulse sequence, the highest generation rate into a single spatial (fiber) mode is  $R_{854, \text{triggered}} = 3.0(6) \text{ kHz}$ .

A first cw interaction measurement is performed using continuous generation of 854 nm photons at the sender ion while monitoring quantum jumps at the receiver ion. It is illustrated by Fig. 3. When the 850 nm laser at the sender is switched off, such that no photons are generated, dark-to-bright fluorescence jumps at the receiver ion mark spontaneous decay of the  $D_{5/2}$  level. From a 20 min fluorescence trace we extract the effective lifetime of the  $D_{5/2}$  level given by the average length of the dark period  $\tau_{\text{off}} = 1022(33) \text{ ms}$ , and the respective decay

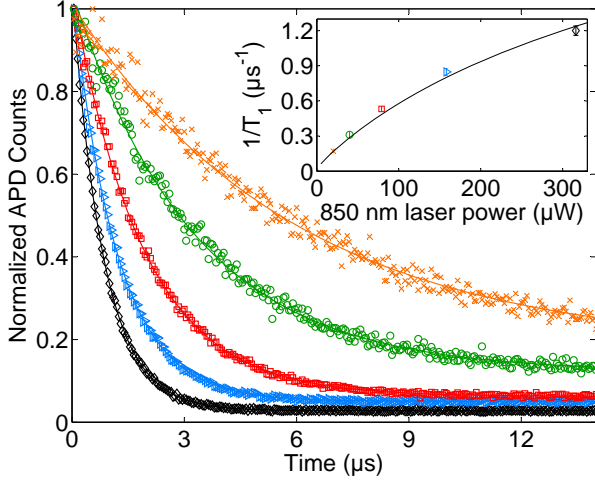


FIG. 2. (Color online) Distribution of single-photon arrival times for various values of 850 nm laser power. Time zero is marked by switching on the 850 nm laser beam. Experimental data are displayed with 50 ns time resolution. The lines are exponential fits to the data from which the photon wave packet durations  $T_1 = \{0.833(3), 1.18(4), 1.88(7), 3.22(27), 5.8(5)\} \mu\text{s}$  are deduced. Each curve corresponds to 15 min of acquisition at a repetition rate of 55.5 kHz (first three curves) resp. 30 kHz (last two curves). The inset shows the inverse wave packet duration  $1/T_1$  as a function of the 850 nm laser power. The solid line is calculated by numerically solving the optical Bloch equations including all Zeeman sublevels.

rate  $R_{\text{off}} = 0.97(3) \text{ s}^{-1}$  (see Fig. 3a). The value of  $\tau_{\text{off}}$  is slightly lower than the literature value of 1168(9) ms [29]; this may be caused by 854 nm background light entering the trap.

When the 850 nm laser at the sender ion is switched on, a significant reduction of the dark period duration to  $\tau_{\text{on}} = 247(6) \text{ ms}$  is observed, corresponding to a decay rate  $R_{\text{on}} = 4.0(1) \text{ s}^{-1}$  (see Fig. 3b). From the two values, we find the absorption rate of 854 nm photons,  $R_{\text{abs}} = R_{\text{on}} - R_{\text{off}} = 3.0(1) \text{ s}^{-1}$ . This rate was measured at about 12 kHz photon transmission rate, hence we conclude that a single photon is absorbed by the receiver ion with  $P_{\text{abs}} = 2.5(5) \cdot 10^{-4}$  probability.

We obtain an independent value for the single-photon absorption probability at the receiver ion by sending photons from a 854 nm cw laser through the same fiber that we use for transmitting the single photons from the sender ion. The laser is attenuated to an intensity that results in about the same APD count rate as for continuous single-photon generation. Under these conditions we find an absorption probability of  $P_{\text{laser}} = 4.3(9) \cdot 10^{-4}$ . We attribute the reduction in the case of single-photon transmission to frequency broadening of the sender photons: while the single-frequency laser is tuned to the peak of the absorption spectrum, the generated single photons have various frequency components, corresponding

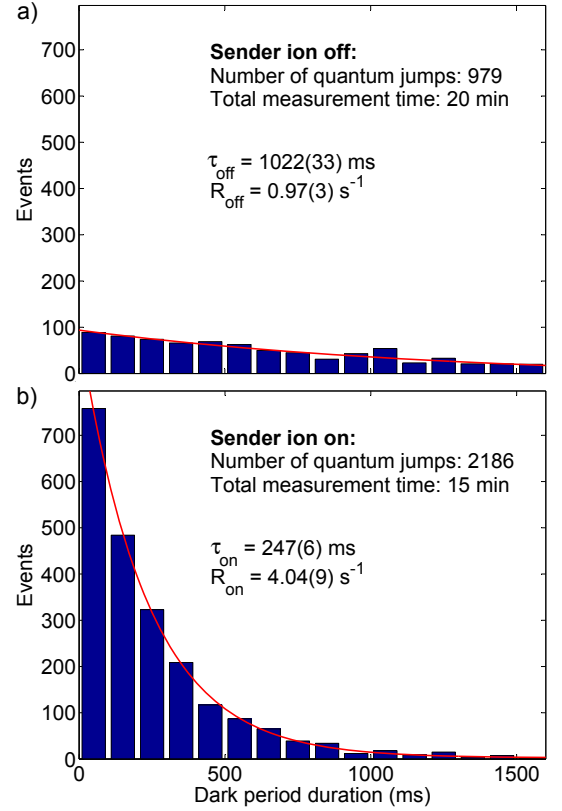


FIG. 3. (Color online) Histogram of dark period durations in the receiver ion after a quantum jump to  $D_{5/2}$ ; a) without photons from the sender ion, and b) with photons continuously transmitted. The mean values of the dark periods  $\tau_{\text{on,off}}$  and the corresponding decay rates  $R_{\text{on,off}} = 1/\tau_{\text{on,off}}$  are also displayed.

to the involved Zeeman transitions; additionally, their rapid generation leads to a spectral width of the individual photons of about 6 MHz. Numerical calculations taking these broadening mechanisms into account confirm the measured reduction within the error margins.

Finally, we transmit triggered single photons from sender to receiver, operating the sender ion in sequence mode. In order to demonstrate that their absorption is signaled by a dark-to-bright quantum jump, we temporally correlate the emission trigger at the sender with the first 397 nm fluorescence photon that we detect at the receiver after a quantum jump. The data are shown in Fig. 4. Trigger-absorption coincidence is evidenced by a peak in the correlation function on top of a background of uncorrelated events. Starting from zero time delay, a steep rise is visible from  $0.8 \mu\text{s}$  to  $1.6 \mu\text{s}$ , reflecting the photon wave packet duration that was set to  $\tau_{854} = 1.1 \mu\text{s}$ . The rise is followed by an exponential decay with  $3 \mu\text{s}$  time constant, corresponding to the average time between absorption and detection of the first photon, i.e. to the inverse of the detection rate of 397 nm photons,  $R_{397} = 3 \cdot 10^5 \text{ Hz}$ . The convolution of these two

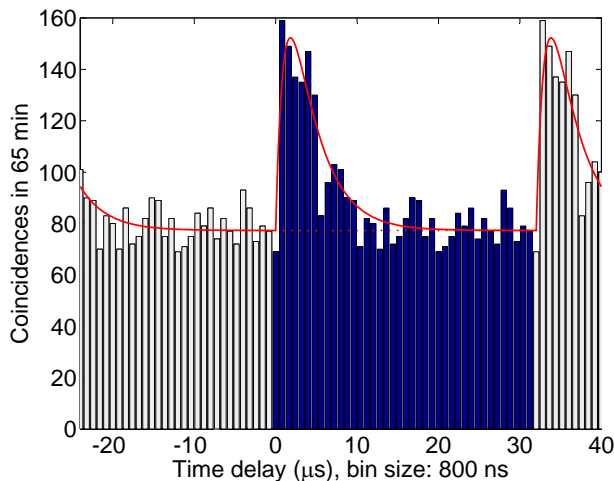


FIG. 4. (Color online) Temporal correlation function (time delay distribution) between single-photon emission triggers at the sender ion and absorption events (quantum jumps) at the receiver ion. These data were recorded with 31.25 kHz sequence repetition rate for a total acquisition time of 65 min, and are displayed with  $0.8 \mu\text{s}$  bin size. The red curve shows the expected dependence, and the dotted line indicates the background level (details see text). The signal repeats with the sequence repetition time (grey areas).

exponentials (red curve in Fig. 4) fits the data very well. The background (dotted line in Fig. 4) of  $\sim 80$  events per  $0.8 \mu\text{s}$  time bin arises from uncorrelated pairs of emission triggers and quantum jumps induced by spontaneous decay of the  $D_{5/2}$  level.

In summary, we generate single-mode 854 nm photons with controlled temporal shape from a single  $^{40}\text{Ca}^+$  ion through resonant three-photon excitation, and we demonstrate their absorption, signaled by a quantum jump, in another ion at  $\sim 1$  m distance. In continuous mode, up to  $1.8 \cdot 10^4$  photons/s are transmitted between the ions, and single-photon absorption results in a reduction to 24% of the  $D_{5/2}$  lifetime at the receiver ion. In sequence mode, the onset of a trigger laser heralds the creation of a transmitted photon, and the correlation function between the emission trigger and the photon absorption signal reveals the coincidence of these processes within the time resolution of about  $3 \mu\text{s}$ , set by the detection rate of fluorescence photons. With 125 kHz sequence repetition frequency, the photon transmission rate is 3 kHz, and about 0.025% of these photons are absorbed in the receiver ion. Taking the emission trigger as a herald for the absorption events, the overall heralding efficiency is  $6 \cdot 10^{-6}$ .

Our experiment is a proof of principle of heralded individual photon absorption in a single atom. In order to preserve the photonic state in the atom and thereby realize a heralded quantum memory, we will combine our method with the detection of the Raman-scattered photon created in the absorption process, which we recently

demonstrated with 1.5% efficiency [25]. This will also make the heralding independent of the emission trigger, thereby allowing for, e.g., entanglement transfer between photon and atom pairs [30]. Among the systems with which single-photon absorption by a single absorber has been observed [16–18], single ions stand out for their unique prospect of integrating atom-photon interfaces with multi-qubit quantum logic. The results also offer the perspective of photonic interaction between different single quantum systems in a hybrid quantum network, e.g. between ions and solid-state emitters or absorbers [31], possibly assisted by quantum frequency conversion [32] to bridge the gap between different wavelengths.

We acknowledge support by the BMBF (Verbundprojekt QuOREP, CHIST-ERA project QScale), the German Scholars Organization/Alfried Krupp von Bohlen und Halbach-Stiftung, the EU (AQUITE Integrating Project) and the ESF (IOTA COST Action).

---

\* mschug@physik.uni-saarland.de

- [1] H. J. Kimble, *Nature* **453**, 1023 (2008).
- [2] J. I. Cirac, P. Zoller, H. J. Kimble, and H. Mabuchi, *Phys. Rev. Lett.* **78**, 3221 (1997).
- [3] P. Grangier, B. Sanders, and J. Vuckovic, *New. J. Phys.* **6**, (2004).
- [4] A. Kuhn, M. Hennrich and G. Rempe, *Phys. Rev. Lett.* **89**, 067901 (2002).
- [5] J. McKeever, A. Boca, A. D. Boozer, R. Miller, J. R. Buck, A. Kuzmich, H. J. Kimble, *Science* **303**, 1992 (2004).
- [6] M. Keller, B. Lange, K. Hayasaka, W. Lange, and H. Walther, *Nature* **431**, 1075 (2004).
- [7] H. G. Barros, A. Stute, T. E. Northup, C. Russo, P. O. Schmidt, and R. Blatt, *New J. Phys.* **11**, 103004 (2009).
- [8] P. Michler, A. Kiraz, C. Becher, W. V. Schoenfeld, P. M. Petroff, L. Zhang, E. Hu, and A. Imamoglu, *Science* **290**, 2282 (2000).
- [9] A. Beveratos, S. Kühn, R. Brouri, T. Gacoin, J.-P. Poizat and P. Grangier, *Eur. Phys. J. D* **18**, 191 (2002).
- [10] B. B. Blinov, D. L. Moehring, L.-M. Duan, and C. Monroe, *Nature (London)* **428**, 153 (2004).
- [11] J. Volz, M. Weber, D. Schlenk, W. Rosenfeld, J. Vrana, K. Saucke, C. Kurtsiefer, and H. Weinfurter, *Phys. Rev. Lett.* **96**, 030404 (2006).
- [12] T. Wilk, S. C. Webster, A. Kuhn, and G. Rempe, *Science* **317**, 488 (2007).
- [13] A. Stute, B. Casabone, P. Schindler, T. Monz, P. O. Schmidt, B. Brandstätter, T. E. Northup, and R. Blatt, *Nature (London)* **485**, 482 (2012).
- [14] N. Piro, F. Rohde, C. Schuck, M. Almendros, J. Huwer, J. Ghosh, A. Haase, M. Hennrich, F. Dubin, and J. Eschner, *Nat. Phys.* **7**, 17 (2011).
- [15] J. Huwer, J. Ghosh, N. Piro, M. Schug, F. Dubin, and J. Eschner, *New J. Phys.* **15**, 025033 (2013).
- [16] Y. L. A. Rezus, S. G. Walt, R. Lettow, A. Renn, G. Zumofen, S. Götzinger, and V. Sandoghdar, *Phys. Rev.*

- Lett. **108**, 093601 (2012).
- [17] H. P. Specht, C. Nölleke, A. Reiserer, M. Uphoff, E. Figueroa, S. Ritter, and G. Rempe, *Nature (London)* **473**, 190 (2011).
  - [18] S. Ritter, C. Nölleke, C. Hahn, A. Reiserer, A. Neuzner, M. Uphoff, M. Mücke, E. Figueroa, J. Bochmann, and G. Rempe, *Nature (London)* **484**, 195 (2012).
  - [19] D. L. Moehring, P. Maunz, S. Olmschenk, K. C. Younge, D. N. Matsukevich, L.-M. Duan, and C. Monroe, *Nature* **449**, 68 (2007).
  - [20] J. Hofmann, M. Krug, N. Ortegel, L. Gérard, M. Weber, W. Rosenfeld, and H. Weinfurter, *Science* **337**, 72 (2012).
  - [21] H.-J. Briegel, W. Dür, J. I. Cirac, and P. Zoller, *Phys. Rev. Lett.* **81**, 5932 (1998).
  - [22] S. V. Polyakov, A. Muller, E. B. Flagg, A. Ling, N. Bjork, E. Van Keuren, A. Migdall, and G. S. Solomon, *Phys. Rev. Lett.* **107**, 157402 (2011).
  - [23] C. Zipkes, L. Ratschbacher, S. Palzer, C. Sias, and M. Köhl, *J. Phys. Conf. Ser.*, **264**, 012019 (2011).
  - [24] M. Almendros, J. Huwer, N. Piro, F. Rohde, C. Schuck, M. Hennrich, F. Dubin, and J. Eschner, *Phys. Rev. Lett.* **103**, 213601 (2009).
  - [25] C. Kurz, J. Huwer, M. Schug, P. Müller, and J. Eschner, *New J. Phys.* **15**, 055005 (2013).
  - [26] S. Gerber, D. Rotter, M. Hennrich, R. Blatt, F. Rohde, C. Schuck, M. Almendros, R. Gehr, F. Dubin, and J. Eschner, *New J. Phys.* **11**, 013032 (2009).
  - [27] R. Gerritsma, G. Kirchmair, F. Zähringer, J. Benhelm, R. Blatt, and C. F. Roos, *Eur. Phys. J. D* **50**, 13 (2008).
  - [28] Assuming saturated occupation (i.e. 50%) of the  $P_{3/2}$  level, and taking into account its lifetime of 6.9 ns and its branching ratio into  $D_{5/2}$  of 5.87% [27], the minimum possible duration of the 854 nm photon wave packet is 236 ns.
  - [29] A. Kreuter, C. Becher, G. P. T. Lancaster, A. B. Mundt, C. Russo, H. Häffner, C. Roos, W. Hänsel, F. Schmidt-Kaler, R. Blatt, and M. S. Safronova, *Phys. Rev. A* **71**, 032504 (2005).
  - [30] N. Sangouard, J.-D. Bancal, P. Müller, J. Ghosh, and J. Eschner, arXiv:1303.6261.
  - [31] E. Neu, R. Albrecht, M. Fischer, S. Gsell, M. Schreck, and C. Becher, *Phys. Rev. B* **85**, 245207 (2012).
  - [32] S. Zaske, A. Lenhard, C. A. Keßler, J. Kettler, C. Hepp, C. Arend, R. Albrecht, W.-M. Schulz, M. Jetter, P. Michler, and C. Becher, *Phys. Rev. Lett.* **109**, 147404 (2012).